9. P. Legault and A. Pardi, *J. Am. Chem. Soc.* **116**, 8390 (1994); *J. Am. Chem. Soc.* **119**, 6621 (1997).
10. A. T. Perrotta, I.-h. Shih, M. D. Been, *Science* **286**, 123 (1999).
11. M. D. Been and G. S. Wickham, *Eur. J. Biochem.* **247**, 741 (1997).
12. T. S. Wadkins, A. T. Perrotta, A. R. Ferré-D'Amaré, J. A. Doudna, M. D. Been, *RNA* **5**, 720 (1999).
13. A. R. Ferré-D'Amaré, K. Zhou, J. A. Doudna, *Nature* **395**, 567 (1998); A. R. Ferré-D'Amaré and J. A. Doudna, *J. Mol. Biol.* **295**, 541 (2000).
14. S. Nakano, D. M. Chadalavada, P. C. Bevilacqua, data not shown.
15. We confirmed that the C75U genomic ribozyme can be rescued by imidazole. In 10 mM Mg^{2+}, pH 7.0, and 200 mM imidazole, an observed rate constant of 0.12 min^{-1} was found.
16. K. B. Schowen and R. L. Schowen, *Methods Enzymol.* **87**, 551 (1982); J. H. Shim and S. J. Benkovic, *Biochemistry* **38**, 10024 (1999).
17. A. J. Kirby and M. Younas, *J. Chem. Soc. B*, 510 (1970); *J. Chem. Soc. B*, 1165 (1970); M. Oivanen, S. Kuusela, H. Lonnberg, *Chem. Rev.* **98**, 961 (1998).
18. D. Herschlag, F. Eckstein, T. R. Cech, *Biochemistry* **32**, 8312 (1993).
19. S. C. Dahm, W. B. Derrick, O. C. Uhlenbeck, *Biochemistry* **32**, 13040 (1993).
20. Y. A. Suh, P. K. Kumar, K. Taira, S. Nishikawa, *Nucleic Acids Res.* **21**, 3277 (1993).
21. A. Hampel and J. A. Cowan, *Chem. Biol.* **4**, 513 (1997); S. Nesbitt, L. A. Hegg, M. J. Fedor, *Chem. Biol.* **4**, 619 (1997); K. J. Young, F. Gill, J. A. Grasby, *Nucleic Acids Res.* **25**, 3760 (1997).
22. Dixon plots of $[k_{obs}(min^{-1})]^{-1}$ versus $[Co(NH_3)_6]^{3+}$, in 2 and 10 mM Mg^{2+}, pH 7.0, yielded straight lines that intersect above the $[Co(NH_3)_6]^{3+}$ axis. This behavior is consistent with competitive inhibition, and revealed an inhibition constant K_i of 45 ± 10 μM for $[Co(NH_3)_6]^{3+}$ [I. H. Segel, *Enzyme Kinetics* (Wiley, New York, 1993)]. The $K_{D,Mg^{2+}}$ at pH 7.0 is 2.4 mM (Fig. 5B). Tighter binding of $[Co(NH_3)_6]^{3+}$ may be due to electrostatic considerations. Similar relative affinities were noted for binding of these ions to the hairpin ribozyme [K. J. Hampel, N. G. Walter, J. M. Burke, *Biochemistry* **37**, 14672 (1998)]. Also, reaction in 10 mM $[Co(NH_3)_6]^{3+}$ was rescued by lowering the pH from 7.0 to 5.0 ($k_{obs} = 3.6 \times 10^{-3}$ min^{-1}) (*14*), as was the case with monovalent ions (Fig. 4A); this result supports native-like folding of the ribozyme in $[Co(NH_3)_6]^{3+}$.
23. R. Basolo and R. G. Pearson, *Mechanisms of Inorganic Reactions* (Wiley, New York, 1988); H. Suga, J. A. Cowan, J. W. Szostak, *Biochemistry* **37**, 10118 (1998).
24. J. H. Cate *et al.*, *Science* **273**, 1678 (1996); J. H. Cate and J. A. Doudna, *Structure* **4**, 1221 (1996); J. H. Cate, R. L. Hanna, J. A. Doudna, *Nature Struct. Biol.* **4**, 553 (1997).
25. I.-h. Shih and M. D. Been, *RNA* **5**, 1140 (1999).
26. It has been suggested that the HDV ribozyme cannot be rescued by high concentrations of monovalent metal ions [J. B. Murray, A. A. Seyhan, N. G. Walter, J. M. Burke, W. G. Scott, *Chem. Biol.* **5**, 587 (1998)]. However, those authors reported a rate constant at pH 8 in the presence of 4 M Li^+ and 25 mM EDTA, which is slower than that observed here (at pH 8.0 in the presence of 1 M Na^+ and 1 mM EDTA) by a factor of only 3.6.
27. Because the transition state appears to be dominated by bond formation to the leaving group (*17*), the general base could be a poor base such as 55 M solvent water ($pK_a = -1.7$), a neighboring phosphate ($pK_a \sim 1$), or a ring nitrogen ($pK_a \sim 4$), which could partially deprotonate the 2′-hydroxyl in the transition state. Increasing the concentration of Hepes from 25 to 50 mM or that of EDTA from 1 to 2 mM did not affect the reaction rate in 1 M NaCl, which suggests that the buffer is not acting as the general base. Between pH 8 and 9, the profile is nearly independent of pH (Fig. 4A), which suggests that specific base catalysis by hydroxide ion may contribute in this regime.
28. V. K. Misra and D. E. Draper, *Biopolymers* **48**, 113 (1998).
29. B. W. Pontius, W. B. Lott, P. H. von Hippel, *Proc. Natl. Acad. Sci. U.S.A.* **94**, 2290 (1997).
30. F. da Silva and R. J. P. Williams, *The Biological Chemistry of the Elements* (Oxford Univ. Press, Oxford, 1993).
31. D. E. Schmidt Jr. and F. H. Westheimer, *Biochemistry* **10**, 1249 (1971).
32. The observed rate constant in saturating Mg^{2+} (50 mM) at pH 5.0 is 0.01 s^{-1} (Fig. 5A). At pH 5.0, the fraction of C75 in the functional protonated state is ~1. The fraction of the magnesium ion in the functional unprotonated state is dependent on the pK_a of the ribozyme-bound $[M(OH)]^+$ used in the calculation. The 50 mM Mg^{2+} data in Fig. 5A suggest that the pK_a for $[Mg(H_2O)_6]^{2+}$ is >9, whereas the unperturbed pK_a of $[Mg(H_2O)_6]^{2+}$ is 11.4 (*19*). Using the slope of 1 in Fig. 5A, the rate constant for chemistry is estimated at 10^2 to 10^4 s^{-1} (~ 0.01 $s^{-1} \times 10^{(pK_a-5)}$). The maximal cleavage rate for RNase A is 1.4×10^3 s^{-1} at 25°C [J. E. Thompson and R. T. Raines, *J. Am. Chem. Soc.* **116**, 5467 (1994)]. The rate constant for the chemical step in the *Tetrahymena* ribozyme has been estimated at 6 s^{-1} at 50°C [D. Herschlag and T. R. Cech, *Biochemistry* **29**, 10159 (1990)].
33. D. Chadalavada, S. Knudsen, S. Nakano, P. C. Bevilacqua, in preparation.
34. A plasmid containing a T7 promoter and the template for the ribozyme was constructed by overlap extension and cloning into pUC19. Mutants were prepared using QuikChange (Stratagene). All DNA constructs were confirmed by dideoxy sequencing. The sequence for the ribozyme is based on a human isolate in which position 85 is a G [S. Makino *et al.*, *Nature* **329**, 343 (1987)]. RNA was transcribed, gel-purified, and 5′–end-labeled by standard methods. RNA was renatured at 55°C for 10 min in 0.5 mM tris (pH 7.5) and 0.05 mM EDTA, then placed at room temperature for 10 min. A saturating concentration (10 μM final) of a DNA oligomer, AS1 [stored in 10 mM tris and 1 mM EDTA (pH 7.5)], which sequesters an inhibitory stretch upstream of the cleavage site (*33*), was added, followed by addition of buffer. The buffer was 25 mM MES (for experiments at pH 4.5 to 6.5) or 25 mM Hepes (for experiments at pH 6.75 to 9.0). Similar kinetics were obtained upon adding small amounts of NaCl (50 mM) (pH 5.0 and 7.0) or changing the buffer to MOPS (pH 6.0 and 7.0) or BICINE (pH 8.0, 8.5, and 9.0). The experimental pH range was limited to 4.5 to 9.0 to avoid ionizing ring nitrogens with pK_as outside of this range (*7*). Water used in the reactions was deionized by a Millipore system. The pH was determined at room temperature and corrected for the slight temperature dependence of buffer pK_a [N. E. Good *et al.*, *Biochemistry* **5**, 467 (1966)]. This mixture was incubated at 37°C for 2 min, a zero time point was removed, and the reaction was initiated by addition of metal ions and performed at 37°C. Depending on the experiment, one of the following salts was added: $MgCl_2$, $CaCl_2$, $CoCl_2$, $Co(NH_3)_6Cl_3$, or NaCl and 1 mM EDTA. Selected reactions were also initiated by AS1 addition, and similar results were obtained. Quenching at various time points was done by addition of an equal volume of a solution of 20 mM EDTA and 90% formamide to ≤10 mM Mg^{2+} solutions, or 100 mM EDTA and 90% formamide to 50 mM Mg^{2+} solutions, and the contents were immediately placed on dry ice. Reactions were separated on a 10% polyacrylamide gel containing 7 M urea, then quantitated on a PhosphorImager (Molecular Dynamics).
35. T. E. Ferrin, C. C. Huang, L. E. Jarvis, R. Langridge, *J. Mol. Graphics* **6**, 13 (1988).

36. Supported by NIH grant GM58709. We thank S. Benkovic, M. Bollinger, S. Booker, T. Glass, and members of the Bevilacqua lab for reading the manuscript before publication and for helpful comments, and S. Tan for assistance in preparing Fig. 3B.

16 November 1999; accepted 27 December 1999

Translocation of *Helicobacter pylori* CagA into Gastric Epithelial Cells by Type IV Secretion

Stefan Odenbreit, Jürgen Püls, Bettina Sedlmaier, Elke Gerland, Wolfgang Fischer, Rainer Haas*

The Gram-negative bacterium *Helicobacter pylori* is a causative agent of gastritis and peptic ulcer disease in humans. Strains producing the CagA antigen (*cagA*$^+$) induce strong gastric inflammation and are strongly associated with gastric adenocarcinoma and MALT lymphoma. We show here that such strains translocate the bacterial protein CagA into gastric epithelial cells by a type IV secretion system, encoded by the *cag* pathogenicity island. CagA is tyrosine-phosphorylated and induces changes in the tyrosine phosphorylation state of distinct cellular proteins. Modulation of host cells by bacterial protein translocation adds a new dimension to the chronic *Helicobacter* infection with yet unknown consequences.

The Gram-negative bacterium *Helicobacter pylori* (*Hp*) colonizes the human gastric epithelium and is strongly associated with peptic ulceration, MALT-lymphoma, and adenocarcinoma of the stomach (*1*). The *cag*A gene is a genetic marker for a 40-kb pathogenicity island (*cag*-PAI) of *Hp*, present in certain strains (*cag*$^+$, type I), but not in others (*cag*$^-$, type II) (*2*). The function of the immunodominant CagA protein is unknown. Attachment of *Hp* to epithelial cells in vitro induces tyrosine phosphorylation of a 145-kD host cell protein (*3*). Mutations in several genes of the *cag*-PAI interfere with tyrosine phosphorylation and secretion of the chemokine interleukin-8 (*4*, *5*). The *cag*-PAI carries a set of genes with homology to so-called type IV secretion systems (*6*), the prototype of which is the *Agrobacterium tumefaciens*

vir operon, which mediates transfer of T-DNA into the nucleus of plant cells (*7*). Several large conjugative plasmids harbor a homologous system, involved in transfer of plasmid DNA into recipient cells during conjugation (*8*). *Bordetella pertussis* uses a similar secretion system for the export of its major proteinaceous virulence factor, the pertussis toxin (*8*). For the postulated *cag* secretion system of *Hp* it was unclear whether DNA or proteins are the target for secretion. Here we provide evidence that the *cag* system is involved in protein secretion.

In agreement with published data (*5*), we show that certain *cag*$^+$ *Hp* strains (P1, P2, P3, P12, G27, and ATCC43526) induce a de novo tyrosine phosphorylation of a protein in AGS epithelial cells (*9*, *10*) (Fig. 1A). The apparent size of this tyrosine-phosphorylated protein varied significantly between different *Hp* isolates (125 to 140 kD), suggesting that it is a size-variable bacterial protein, rather than a host cell protein. Because the size variation of the bacterial protein CagA is in the same range (Fig. 1B), we constructed and tested isogenic *cag*A knockout mutants of *Hp* strains P1 and P12 (*11*). Both mutant strains were unable to induce tyrosine phosphorylation, whereas the wild-type (WT) strains did (Fig. 1, C and D). Knockout mutants in *cagE*, which have a defect in the secretion apparatus, still produced CagA, but lost the tyrosine phosphorylation capability (Fig. 1, C and D). Thus, CagA might be the observed tyrosine-phosphorylated protein translocated into AGS cells by the type IV secretion system.

To verify this hypothesis, we subjected a lysate of AGS cells infected with *Hp* P12 to immunoprecipitation with antiserum to CagA (anti-CagA, AK257) (*12*, *13*). CagA was precipitated when strong denaturing conditions, disrupting membrane structures, were applied (RIPA-buffer) (*12*). The mild detergent Triton X-100, however, resulted in only tiny amounts of immunoprecipitated CagA, arguing for a tight association of a defined CagA pool with subcellular structures of AGS cells. The precipitated protein reacted with both anti-CagA and anti-phosphotyrosine (Fig. 1, E to G, lane 4). Thus, CagA is the tyrosine-phosphorylated protein that is induced by *Hp* attachment, named CagA$^{P\text{-}Tyr}$. In gastric (KatoIII, St 3051) and nongastric (ME180, but not HeLa and Chang) human epithelial cell lines (*9*), CagA$^{P\text{-}Tyr}$ was identified upon attachment of *Hp* P1 and P12.

Next, we examined whether CagA phosphorylation can be inhibited. Staurosporine, a serine-threonine kinase inhibitor, did not have a detectable effect, but genistein, a phosphotyrosine kinase (PTK) inhibitor, blocked CagA phosphorylation completely (*10*) (Fig. 1, H and I), indicating that a eukaryotic-type PTK activity phosphorylates CagA. The phosphotyrosine-specific YopH phosphatase of *Yersinia* completely removed the tyrosine phosphorylation from CagA$^{P\text{-}Tyr}$, demonstrating that phosphorylation of CagA is reversible and tyrosine-specific (Fig. 1, H and I).

To obtain further, direct biochemical evidence for the residence of CagA$^{P\text{-}Tyr}$ in the eukaryotic cell, we established a lysis procedure, based on the detergent saponin, that destroys AGS cells, but leaves *Hp* intact (*14*). Selective lysis of AGS cells released high amounts of CagA$^{P\text{-}Tyr}$ when *cag*A$^+$ WT strains attached, but no CagA$^{P\text{-}Tyr}$ was released from the P12(*cag*E$^-$) knockout mutant or the P12 strain without epithelial cell contact (Fig. 2, A and C). The P12(*cag*E$^-$) mutant strain occasionally released tiny amounts of nonphosphorylated CagA into the supernatant. The soluble cytoplasmic *Hp* RecA protein served as a control, demonstrating that the saponin lysis procedure did not release cytoplasmic proteins from *Hp* (Fig. 2, E and F). The assay shows that a functional type IV secretion system is necessary for translocation of CagA into AGS cells, where it is converted into CagA$^{P\text{-}Tyr}$.

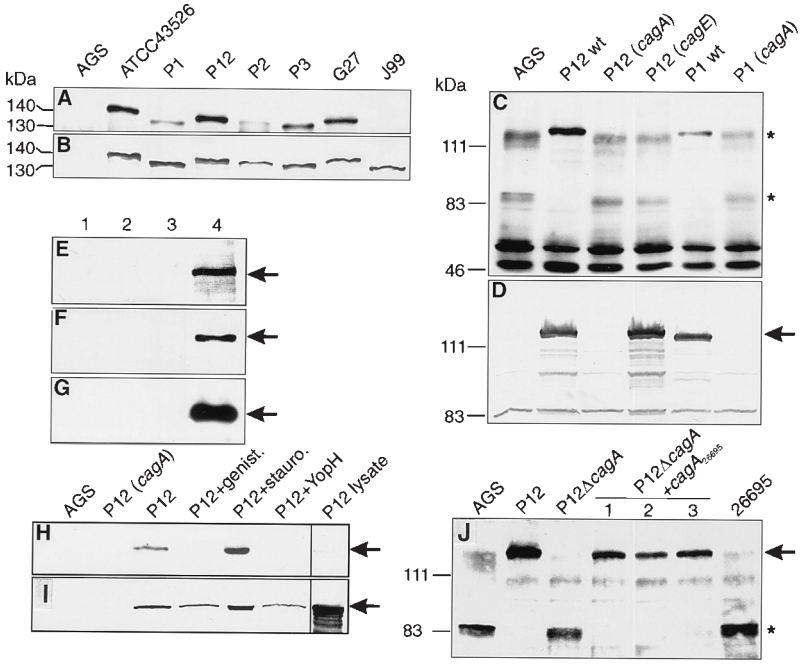

Fig. 1. Tyrosine phosphorylation of *Hp* CagA. (**A** to **D**) Immunoblots showing tyrosine phosphorylation of CagA upon attachment of *Hp* WT (A and B) or isogenic knockout mutant strains (C and D) to AGS epithelial cells. Blots were reacted with anti-phosphotyrosine antibody PY99 (A and C) or anti-CagA (AK257) (B and D). (**E** to **G**) Immunoprecipitation of CagA from a lysate of AGS cells alone (lanes 1 and 2) or AGS cells infected with *Hp* P12 (lanes 3 and 4). AK257 was used for precipitation (lanes 2 and 4); controls without antibody (lanes 1 and 3) (*13*). (E) Silver-stained gel of the precipitate, (F) immunoblot with PY99, and (G) immunoblot with AK257. (**H** and **I**) Protein kinase inhibitor genistein but not staurosporine blocks tyrosine phosphorylation of CagA, and YopH (*10*) dephosphorylates CagA$^{P\text{-}Tyr}$, as demonstrated by PY99 (H) or AK257 (I) in the immunoblot. The P12 lysate was prepared without contact of *Hp* to AGS cells, and the faint band in this lane is not sensitive to genistein treatment. (**J**) Genetic complementation of the P12Δ*cagA* mutant with the Hp 26695 *cagA* gene in trans (lanes 1, 2, and 3 are independent clones). Arrows indicate full-length CagA. Asterisks mark the position of cellular proteins p120-130 and p85 dephosphorylated upon translocation of CagA.

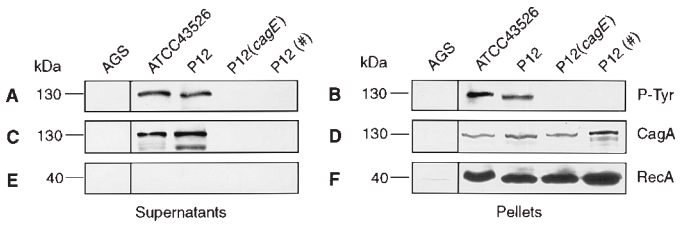

Fig. 2. Selective lysis of AGS cells and release of translocated CagA$^{P\text{-}Tyr}$. Supernatant- (**A**, **C**, and **E**) and pellet (**B**, **D**, and **F**) fractions obtained after selective lysis of AGS cells infected with *Hp* (*10*) were analyzed by immunoblotting with anti-phosphotyrosine mAb PY99 (A and B), anti-CagA (AK257) (C and D), and anti-RecA (AK263) (E and F). (#) P12 without AGS cells.

Max von Pettenkofer Institute for Hygiene and Medical Microbiology, Ludwig-Maximilians University Munich, D-80336 Munich, Germany.

*To whom correspondence should be addressed at Max von Pettenkofer Institute, Pettenkoferstrasse 9a, D-80336 Munich, Germany. E-mail: haas@m3401.mpk.med.uni-muenchen.de

A second, independent approach that we used to demonstrate the presence of CagA in AGS cells was immunofluorescence (IF) (*10*). Anti-CagA (AK257) did not specifically recognize native CagA, and therefore a P12 strain with a precise deletion of *cag*A (P12Δ*cag*A) was constructed and complemented with a COOH-terminally FLAG-tagged version of the 26695 *cag*A gene (*cag*A-FLAG), expressed from the shuttle plasmid pHel2 (*11*). Successful translocation of CagA-FLAG into AGS cells was verified by selective lysis. IF of *Hp* attached to AGS cells revealed staining of *Hp* P12 with anti-*Hp* (AK175, green) and of CagA-FLAG with anti-FLAG M2 monoclonal antibody (mAb) (red) (Fig. 3A). Attached *Hp* translocate CagA-FLAG, which accumulates in the cell close to the attachment site of *Hp*. *Hp*-associated CagA-FLAG was detected only at zones of intimate contact between *Hp* and AGS cells (Fig. 3A, arrows), but not in intact *Hp* without AGS cell contact or the P12 WT strain (Fig. 3B).

Under standard growth conditions, several proteins are tyrosine-phosphorylated in AGS cells (*9*). These include a prominent but diffuse band between 120 and 130 kD (p120-130) and in the 85-kD range (p85), as well as several smaller proteins (Fig. 1C, lane AGS). Attachment of *Hp* strains causes a reduction in the intensity, or even a complete loss, of p120-130 and p85, concomitantly with the appearance of $CagA^{P\text{-}Tyr}$ (Fig. 1, C and J). The rapid (5 to 10 min) disappearance of both protein bands in a time-course experiment suggests a dephosphorylation of these proteins, rather than a blocking of de novo phosphorylation. This effect was not observed when *cag*E^- or *cag*A^- mutants were used for attachment (Fig. 1C), indicating that translocation of CagA and its conversion into $CagA^{P\text{-}Tyr}$ is the causative step for the dephosphorylation of cellular proteins.

To examine why *Hp* 26695, carrying two putative tyrosine phosphorylation sites in CagA (Fig. 4), did not induce $CagA^{P\text{-}Tyr}$, we complemented the P12Δ*cag*A strain by the intact *cag*A gene of *Hp* 26695 in trans, using the pHel2 shuttle vector (*15*). The P12Δ*cag*A deletion mutant induced neither tyrosine phosphorylation of CagA, nor dephosphorylation of host proteins, but the complemented strain restored both activities (Fig. 1J). Thus, the genetic background of P12 allows translocation of the *Hp* 26695 CagA, suggesting that the type IV secretion apparatus in the *Hp* 26695 isolate might be switched off or defective.

A MOTIF databank search (*16*) identified several putative tyrosine phosphorylation motifs in the CagA protein sequence of independent strains (Fig. 4) (*17*). The CagA protein of strain J99 without a motif (*18*) was not tyrosine-phosphorylated (Figs. 1A and 4). The two available *Hp* genome sequences (*18*, *19*) do not contain genes homologous to bacterial or eukaryotic tyrosine kinases, as is the case in other bacteria (*20*, *21*), which supports our hypothesis that CagA is phosphorylated in the eukaryotic cell. Whether translocated CagA induces a cellular protein tyrosine phosphatase (PTP), or whether $CagA^{P\text{-}Tyr}$ itself is a type of eukaryotic PTP is unclear. The identification of CagA as a protein that is translocated into human gastric cells by the type IV secretion apparatus of *Hp* may have important biological consequences for the chronically persisting pathogen, as well as for the host.

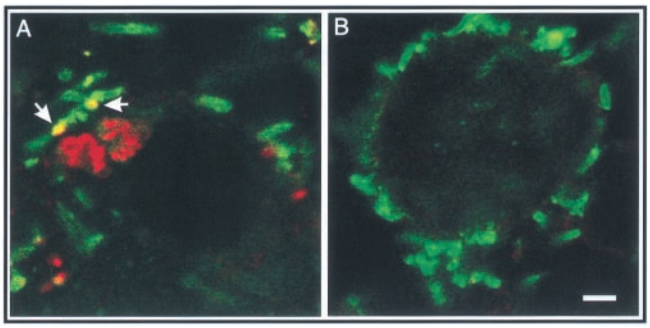

Fig. 3. Immunofluorescence of *Hp* P12Δ*cag*A (*cag*A-FLAG) and *Hp* P12 WT attached to AGS cells. (**A**) Detection of CagA-FLAG by anti-FLAG mAb M2 (red), specific for the FLAG epitope. AK175, directed against *Hp*, reacts with the bacteria (green). CagA-FLAG is detected only at positions of close contact between *Hp* and AGS cells (arrows). (**B**) P12 WT strain attaching to AGS cells reacts with AK175 (green) but not with M2 (red). Bar, 2 μm.

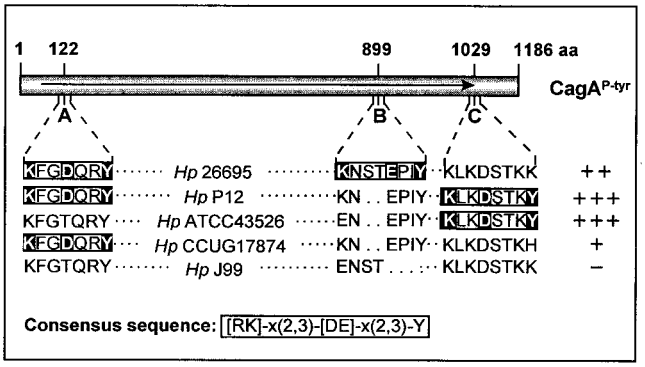

Fig. 4. Putative tyrosine phosphorylation motifs in CagA and phosphorylation intensity of variant CagA proteins. Schematic representation of the *Hp* 26695 CagA sequence and three putative tyrosine phosphorylation sites A, B, and C in different sequences. The eukaryotic tyrosine phosphorylation consensus sequence and putative motifs in the CagA sequences are boxed, conserved amino acids are shown in outline. Y denotes the phosphorylated tyrosine residue. aa, amino acid position. (+) low, (++) medium, (+++) strong, (−) no tyrosine phosphorylation of CagA. Abbreviations for the amino acid residues are as follows: D, Asp; E, Glu; F, Phe; G, Gly; H, His; I, Ile; K, Lys; L, Leu; N, Asn; P, Pro; Q, Gln; R, Arg; S, Ser; T, Thr; and Y, Tyr.

References and Notes

1. M. J. Blaser, *Sci. Am.* **274** 104 (February 1996).
2. Z. Y. Xiang *et al.*, *Infect. Immun.* **63**, 94 (1995).
3. E. D. Segal, S. Falkow, L. S. Tompkins, *Proc. Natl. Acad. Sci. U.S.A.* **93**, 1259 (1996).
4. S. Censini *et al.*, *Proc. Natl. Acad. Sci. U.S.A.* **93**, 14648 (1996).
5. E. D. Segal, C. Lange, A. Covacci, L. S. Tompkins, S. Falkow, *Proc. Natl. Acad. Sci. U.S.A.* **94**, 7595 (1997).
6. A. Covacci, J. L. Telford, G. Del Giudice, J. Parsonnet, R. Rappuoli, *Science* **284**, 1328 (1999).
7. K. J. Fullner, J. C. Lara, E. W. Nester, *Science* **273**, 1107 (1996).
8. S. C. Winans, D. L. Burns, P. J. Christie, *Trends. Microbiol.* **4**, 64 (1996).
9. Bacterial strains P1, P2, P3, P12 have been described (*22*). Strains 26695, J99, ATCC43526, and NCTC11637 are reference strains obtained from the American Type Culture Collection (ATCC). Human gastric cell lines AGS (ATCC CRL 1739), KatoIII (ATCC HTB103), St 3051, or nongastric epithelial cell lines ME180 (ATCC HTB 33), HeLa (ATCC CCL 2), or Chang (ATCC CCL 20.2) were grown in RPMI 1640 medium (Gibco) containing 10% fetal calf serum and L-glutamine in a water-saturated atmosphere at 37°C and 5% CO_2.
10. For infection experiments, cells were grown in a preconfluent monolayer (5×10^5 cells) and infected with bacteria at a multiplicity of infection (MOI) of 100 for 4 hours at 37°C and 5% CO_2. Nonadherent bacteria were removed by washing five times with PBS* [phosphate-buffered saline (PBS), 1 mM $CaCl_2$, 0.5 mM $MgCl_2$]. Cells were suspended in 1 ml of ice-cold PBS* (PBS, 1 mM EDTA, 1 mM orthovanadate, 1 mM phenylmethylsulfonyl fluoride (PMSF), 1 μM leupeptin, 1 μM pepstatin) (cell scraper), collected by centrifugation, and resuspended in 30 μl PBS*. For kinase inhibition studies, the cell culture medium was supplemented with 250 μM genistein or 1 μM staurosporine 1 hour before and during infection. For dephosphorylation, cells were collected in 30 μl of PBS, 0.1% Triton X-100 and incubated with 50 U of YopH phosphatase (NEB) for 1 hour at 30°C. For SDS–polyacrylamide gel electrophoresis, 40 μl of a twofold sample solution were added before boiling (5 min). Proteins were separated on a 6% polyacrylamide gel, blotted on a polyvinylidene difluoride membrane, and examined for CagA (AK257, protein A/AP) or tyrosine phosphorylation (PY99, Santa Cruz Biotechnology; anti-mouse immunoglobulin G (IgG)–horseradish peroxidase (HRP). The HRP-conjugated antibody was visualized by enhanced chemiluminescence (Renaissance, NEN). For immunofluorescence studies, AGS cells were grown to a preconfluent state and infected with *Hp* at a MOI of 100 for 3 hours. After removal of nonadherent bacteria, cells were fixed in 3.7% paraformaldehyde and permeabilized with 0.1% Triton X-100. *Hp* was detected with AK175 (*13*) and fluorescein isothiocyanate–conjugated anti-rabbit IgG. The FLAG-tagged CagA was

visualized with the FLAG-specific mAb M2 and TRITC-coupled anti-mouse IgG.
11. Plasmid pWS30 (*22*) was used for inactivation of *cag*A. For construction of a *cag*E$^-$ insertion mutant, the *Hp* 26695 chromosomal region (position 574639 to 579587) was amplified by polymerase chain reaction (PCR). The PCR fragment was cloned in pMin1, mutated by a Tn*Max* transposon derivative as described [A. F. Kahrs *et al.*, *Gene* **167**, 53 (1995)], and used for transformation of strain P12, resulting in the *cag*E$^-$ mutant. For construction of P12Δ*cag*A, region 579021 –to 579905 (*cag*A-upstream) and 583483 to 584934 (*cag*A-downstream) of the Hp 26695 genome were amplified by PCR with 18-nucleotide flanking sequences as primers. Fragments were cloned into pBluescript Xho I–Bam HI sites, separated by an *aph*A-3 gene cassette. For complementation, the *cag*A gene of 26695 was amplified by PCR and cloned into the pHel2 vector (Xho I–Bam HI) (*15*). The FLAG-tag (Sigma) sequence was fused to the *cag*A-downstream primer (5′-CGGGATCCTTACTTGTCATCGTCGTCCTTGTAGTCAGATTTTTGGAAACCACCTT-3). The 18-nucleotide *cag*A upstream primer starts at position 579701 (*19*). Transformation of *Hp* strains was performed as described [R. Haas *et al.*, *Mol. Microbiol.* **8**, 753 (1993)].
12. AGS cells (1×10^7) were infected with *Hp* P12, incubated for 4 hours (37°C, 5% CO_2), washed 5× with PBS*, and lysed in 500 μl of modified RIPA buffer [50 mM tris-HCl (pH 7.4), 150 mM NaCl, 1 mM EDTA, 1% NP-40, 0.25% Na-deoxycholate, 1 mM PMSF, 1 mM orthovanadate, 1 μM leupeptin,1 μM pepstatin] (1 hour, 4°C, gentle shaking). The lysate was cleared (15,000 rpm, 4°C, 10 min) and the protein content adjusted to 3 mg/ml with PBS*. AK257 (1.7 μg/ml) was added to a total volume of 900 μl; after 1 hour at 4°C, 40 μl of Protein G–agarose (Roche) was added and the mixture incubated for a further 2 hours at 4°C. After a short centrifugation step (10 s, 6.000*g*) the supernatant was discarded, and beads were washed four times with 1 ml of PBS* and suspended in 40 μl of sample solution.
13. The COOH-terminal part of CagA was produced as a fusion protein with MS2-polymerase and an NH_2-terminal His_6-tag by using the *Escherichia coli* expression vector pEV40 [J. Pohlner *et al.*, *Gene* **130**, 121 (1993)]. The fusion protein was expressed and purified by Ni^{2+}–nitrilotriacetic acid affinity chromatography by standard procedures and used to immunize a rabbit to obtain antiserum AK257. AK175 was generated by immunization of a rabbit with whole heat-killed *Hp* bacteria. Immunoblotting was performed and alkaline phosphatase (AP)–coupled protein A was used to visualize the antibody bound by decomposition of nitro blue tetrazolium.
14. After standard infection of AGS cells with *Hp* strains (*10*), cells were washed three times with PBS$^+$, harvested with a cell scraper, and treated with PBS* containing 0.05% (w/v) saponin for 10 min at room temperature. Cellular debris and bacteria were separated from the soluble material by centrifugation (5 min, 6000*g*) and 0.2-μm pore diameter filtration of the supernatant. Pellets were resuspended in 30 μl of sample solution, and supernatants were precipitated with chloroform-methanol as described [D. Wessel and U. I. Flügge, *Anal. Biochem.* **138**, 141 (1984)] and resuspended in 30 μl of sample solution. Equal amounts (8 μl) of probes were loaded on 6 or 10% polyacrylamide gels.
15. D. Heuermann and R. Haas, *Mol. Gen. Genet.* **257**, 519 (1998).
16. Available at www.motif.genome.ad.jp/.
17. The sequence of the P12*cagA* gene was obtained by PCR amplification of the complete gene fragment from corresponding chromosomal DNA and sequencing of the cloned genes by primer walking. ATCC43526 CagA (GenBank accession number 2073135), CagA sequences of J99 (*18*) and 26695 (*19*).
18. R. A. Alm *et al.*, *Nature* **397**, 176 (1999).
19. J.-F. Tomb *et al.*, *Nature* **388**, 539 (1997).
20. E. E. Galyov, S. Håkansson, A. Forsberg, H. Wolf-Watz, *Nature* **361**, 730 (1993).
21. O. Ilan *et al.*, *EMBO J.* **18**, 3241 (1999).
22. W. Schmitt and R. Haas, *Mol. Microbiol.* **12**, 307 (1994).
23. We thank W.-D. Hardt, M. Aepfelbacher, and J. Heesemann for constructive comments on the manuscript, A. Covacci for the gift of *Hp* strain G27, and K. Melchers for *Hp* strain ATCC43526. Supported by grants from the Deutsche Forschungsgemeinschaft to R.H. (HA 2697/2-1).

9 August 1999; accepted 7 January 2000

Virus-Induced Neuronal Apoptosis Blocked by the Herpes Simplex Virus Latency-Associated Transcript

Guey-Chuen Perng,[1] Clinton Jones,[2] Janice Ciacci-Zanella,[2] Melissa Stone,[2] Gail Henderson,[2] Ada Yukht,[1] Susan M. Slanina,[1] Florence M. Hofman,[3] Homayon Ghiasi,[1,4] Anthony B. Nesburn,[1,4] Steven L. Wechsler[1,4]*

Latent infections with periodic reactivation are a common outcome after acute infection with many viruses. The latency-associated transcript (*LAT*) gene is required for wild-type reactivation of herpes simplex virus (HSV). However, the underlying mechanisms remain unclear. In rabbit trigeminal ganglia, extensive apoptosis occurred with *LAT*$^-$ virus but not with *LAT*$^+$ viruses. In addition, a plasmid expressing *LAT* blocked apoptosis in cultured cells. Thus, *LAT* promotes neuronal survival after HSV-1 infection by reducing apoptosis.

After primary infection of the eye, herpes simplex virus–type 1 (HSV-1) establishes a lifelong latent infection in neurons of the trigeminal ganglia (TGs), with sporadic periods of reactivation and recurrent disease. Recurrent ocular HSV (HSV-1 and HSV-2) is a leading cause of corneal blindness resulting from an infectious agent. Recurrent genital HSV is a serious sexually transmitted disease. Latent HSV infections affect 70 to 90% of adults.

During latency, a single viral gene—the *LAT* gene—is abundantly transcribed (*1, 2*). *LAT* is essential for the efficient reactivation of HSV from latency (*3*). The primary *LAT* is 8.3 kb and overlaps the important immediate early gene *ICP0* in an antisense direction. Thus, it was proposed that *LAT* may function through an antisense mechanism (*1, 2*). However, the first 1.5 kb of LAT alone is sufficient for wild-type levels of spontaneous reactivation (*4*), and this region does not overlap any known HSV-1 gene. *LAT* may enhance the establishment or maintenance of latency (*5–8*), thereby increasing the pool of latently infected neurons, which in turn results in increased levels of spontaneous and/or induced reactivation (*9*). Although studies with one *LAT*$^-$ mutant have suggested that a *LAT*-related function may suppress productive-cycle gene expression during acute and latent infection of mouse trigeminal ganglia (*10, 11*), no evidence was presented to show that *LAT* caused these effects directly, rather than through a pleiotropic effect. We recently reported on a mutant containing a partial deletion of *LAT* in which neurovirulence was increased (*12*). This finding suggested that *LAT* might protect neurons from being killed by HSV-1, thereby allowing HSV-1 to establish latency in more neurons.

To determine whether neurons were being protected by *LAT*, we used dLAT2903, a *LAT* null mutant derived from the McKrae strain of HSV-1 (*3*). This mutant contains a deletion that includes the *LAT* promoter and the 5′ half of the stable 2-kb *LAT*; this deletion (nucleotides −161 to +1667) results in the absence of *LAT* RNAs and does not overlap or interfere with the *ICP0* transcript. Like most *LAT* mutants, dLAT2903 has no known deficits other than being impaired for reactivation from latency. Thus, dLAT2903 is wild type for replication in mouse and rabbit eyes, HSV-1–induced eye disease, replication in TGs, and neurovirulence (*3*). However, with dLAT2903, large numbers of neurons positive for TUNEL (terminal deoxynucleotidyl transferase–mediated deoxyuridine triphosphate nick-end labeling) were seen in rabbit TGs on day 7 after infection (Table 1; 70% of sections, 100% of TGs), whereas in this experiment TUNEL-positive cells were not de-

[1]Ophthalmology Research Laboratories, Cedars-Sinai Medical Center Burns & Allen Research Institute, 8700 Beverly Boulevard, Los Angeles, CA 90048, USA. [2]Department of Veterinary and Biomedical Sciences, Center for Biotechnology, University of Nebraska, Lincoln, NE 68583, USA. [3]Department of Pathology, University of Southern California School of Medicine, Los Angeles, CA 90025, USA. [4]Department of Ophthalmology, UCLA School of Medicine, Los Angeles, CA 90024, USA.

*To whom correspondence should be addressed. E-mail: Wechsler@CSMC.edu